Molecular Cell
Article

DNA Binding Cooperativity of p53 Modulates the Decision between Cell-Cycle Arrest and Apoptosis

Katharina Schlereth,[1,6] Rasa Beinoraviciute-Kellner,[1,2,6] Marie K. Zeitlinger,[1] Anne C. Bretz,[1] Markus Sauer,[1] Joël P. Charles,[1] Fotini Vogiatzi,[1] Ellen Leich,[3] Birgit Samans,[4] Martin Eilers,[5] Caroline Kisker,[2] Andreas Rosenwald,[3] and Thorsten Stiewe[1,*]

[1]Department of Hematology, Oncology, and Immunology, Molecular Oncology, Philipps-University, 35032 Marburg, Germany
[2]Rudolf Virchow Center, DFG Research Center for Experimental Biomedicine, University of Würzburg, 97078 Würzburg, Germany
[3]Institute of Pathology, University of Würzburg, 97080 Würzburg, Germany
[4]Institute of Molecular Biology and Tumor Research, Philipps-University, 35032 Marburg, Germany
[5]Theodor Boveri Institute, Physiological Chemistry, University of Würzburg, 97074 Würzburg, Germany
[6]These authors contributed equally to this work
*Correspondence: thorsten.stiewe@staff.uni-marburg.de
DOI 10.1016/j.molcel.2010.02.037

SUMMARY

p53 limits the proliferation of precancerous cells by inducing cell-cycle arrest or apoptosis. How the decision between survival and death is made at the level of p53 binding to target promoters remains unclear. Using cancer cell lines, we show that the cooperative nature of DNA binding extends the binding spectrum of p53 to degenerate response elements in proapoptotic genes. Mutational inactivation of cooperativity therefore does not compromise the cell-cycle arrest response but strongly reduces binding of p53 to multiple proapoptotic gene promoters (*BAX*, *PUMA*, *NOXA*, *CASP1*). Vice versa, engineered mutants with increased cooperativity show enhanced binding to proapoptotic genes, which shifts the cellular response to cell death. Furthermore, the cooperativity of DNA binding determines the extent of apoptosis in response to DNA damage. Because mutations, which impair cooperativity, are genetically linked to cancer susceptibility in patients, DNA binding cooperativity contributes to p53's tumor suppressor activity.

INTRODUCTION

The tumor suppressor p53 is known as the "guardian of the genome" owing to its central role in an intricate signaling network controlling life and death (Vousden and Lane, 2007). p53 is activated in response to various types of cellular stress, including DNA damage and oncogene activation. As a transcription factor, p53 initiates transcriptional programs that ultimately arrest proliferation and prevent the generation of genetically altered cells. Not surprisingly, defects in the p53 network lead to tumor development and are encountered in the majority of cancer patients either as missense mutations in p53 itself or, alternatively, in genes encoding other components of the p53 network (Stiewe, 2007; Vousden and Lane, 2007).

p53 possesses the classical features of a sequence-specific transcriptional activator, including a transactivation domain at the N terminus, a DNA-binding "core" domain in the center of the protein, and a tetramerization domain at the C terminus. p53 binds as a tetramer in a sequence-specific manner to DNA-binding sites consisting of two decameric motifs or half-sites of the general form RRRCWWGYYY (R = A, G; W = A, T; Y = C, T) separated by 0–14 base pairs (Riley et al., 2008). Depending on the set of target genes activated under a given condition, the outcome of p53 activation is either a transient cell-cycle arrest enabling damage repair, an irreversible block of proliferation by senescence or differentiation, or cell death via apoptosis (Stiewe, 2007; Vousden and Lu, 2002). Whereas cell-cycle arrest depends on the ability of p53 to induce the transcription of target genes such as the CDK inhibitor $p21^{CDKN1A}$, apoptosis depends on the induction of a distinct class of target genes including *BAX*, *PMAIP1* (*NOXA*), *BBC3* (*PUMA*), *P53AIP1*, *FAS*, *FDXR*, and *TP53I3* (*PIG3*). Together with a direct nonnuclear proapoptotic function of p53 in the cytoplasm and mitochondria, these genes promote mitochondrial outer-membrane permeabilization and cytochrome *c* release, leading to the activation of caspases and apoptotic cell death (Chipuk and Green, 2006). The decision between cell-cycle arrest and apoptosis as the two main biological responses initiated by p53 depends strongly on the cellular context and reflects both the concentration and the posttranslational modification state of p53 (Vousden and Lu, 2002). However, the molecular details of how p53 distinguishes between the genes of the different transcriptional programs still remain unclear.

Recent studies combining small-angle X-ray scattering, electron microscopy, and NMR data of full-length p53 with previously solved solution and crystal structures of isolated p53 fragments demonstrated that the intact p53 protein in complex with DNA forms a tetramer that can be described as a symmetric dimer of dimers (Cho et al., 1994; Kitayner et al., 2006; Tidow et al.,

2007). Isolated p53 core domains, although mostly monomeric in solution, bind to DNA as tetramers, indicating cooperative binding supported by protein-protein interactions (Weinberg et al., 2004). The crystal structure of the p53 core domain tetramer reveals two types of protein-protein interfaces: a symmetrical intradimer and a translational interdimer interface (Kitayner et al., 2006). Based on both biochemical and structural studies, the symmetrical interface within each dimer involves the reciprocal interaction of oppositely charged residues (Glu180, Arg181) in helix H1. These residues are evolutionarily conserved in p53 but absent in the p53 family members p63 and p73 (Figures 1A and 1B; see Table S1 available online) (Dehner et al., 2005; Kitayner et al., 2006; Klein et al., 2001; Veprintsev et al., 2006). This interaction between two p53 monomers was found to be crucial for the cooperative nature of DNA binding by isolated recombinant p53 core domains (Dehner et al., 2005). Similarly, in an alternative structure postulated by molecular dynamics simulations on the basis of the asymmetric dimer of the crystal p53-trimer DNA complex (Cho et al., 1994), the four H1 helices form a bundle which is stabilized by circular E180-R181 salt bridges (Ma and Levine, 2007). On the basis of this biochemical and structural evidence for cooperative DNA binding by p53, we here examine the role of DNA binding cooperativity for p53's tumor suppressor activity.

RESULTS

Role of H1 Helix Interactions for In Vitro DNA Binding

To investigate the role of DNA binding cooperativity for p53 function, we introduced modest charge-neutralizing (E180→L "LR" and R181→L "EL") and more severe charge-inverting (E180→R "RR" and R181→E "EE") mutations into the H1 helix of the full-length p53 molecule (Figure 1C). The short names denote the amino acid sequence at positions 180 and 181 in the mutant proteins, for example "ER" for E180,R181 in the wild-type. These point mutations have previously been demonstrated to compromise p53 interactions and thus DNA binding cooperativity in the context of the isolated core domains in vitro (Dehner et al., 2005). To assure that functional defects are truly due to defective core domain interactions and are not caused by structural misfolding of the core domain or disturbed interaction with other cellular proteins, we also introduced the two most severe mutations E180R and R181E together into a single p53 molecule (double mutant E180,R181→R180,E181 "RE") and used the two complementing mutants "EE" and "RR" in functional rescue studies. All H1 helix but not tetramerization domain mutants formed tetramers under native, nondenaturing conditions, indicating that core domain interactions via the H1 helix are not a prerequisite for tetramerization (Figure 1D).

Next, we investigated the impact of H1 helix mutations on DNA binding in the context of the full-length tetrameric p53 molecule by electrophoretic mobility shift assays (EMSAs). Whereas the charge-neutralizing mutations EL and LR had a weak inhibitory effect, the charge-inverting mutations strongly decreased DNA binding to almost undetectable levels in the case of EE (Figure 1E). Importantly, the double mutation RE and the combination of EE and RR restored DNA binding to levels that even exceeded the binding of the wild-type protein. The mutant EE, which was unable to bind DNA on its own, was efficiently recruited into a DNA-bound complex by the complementing mutant RR, as shown by supershift analysis (Figure 1F). To distinguish a role in inter- and intradimer interactions, we further tested the H1 helix mutations in the context of the dimeric L344A tetramerization domain mutant. L344A formed both dimers and tetramers on full sites (20-mers) but only dimers on half-sites (decamers) (Figure 1G). EE and RR in the context of the L344A backbone were both unable to bind half-site DNA. In combination, however, they efficiently bound single half-sites, indicating that these two proteins can complement each other to form a strongly DNA-bound heterodimer, thus proving a role for helix H1 in intradimer versus interdimer interactions. In addition, time-resolved dissociation EMSAs confirmed decreased DNA-protein complex stabilities for the interaction-impaired mutants LR, RR, and EL and increased stabilities for the double mutant RE and the combination of EE+RR (Figures 1H and 1I). The H1 helix therefore not only mediates cooperative DNA binding of isolated p53 core domains but is also crucial in the context of the tetrameric full-length p53 molecule. This allowed us to use H1 helix mutants to investigate the role of DNA binding cooperativity for p53's tumor suppressor activity.

DNA Binding Cooperativity Modulates the Decision between Cell-Cycle Arrest and Apoptosis

Initial data from the H1 helix mutants indicated that p53's antiproliferative activity directly correlated with the interaction strength and thus DNA binding cooperativity (Figures S1A–S1D). p53 exerts its antiproliferative activity by either arresting the cell cycle or inducing rapid apoptotic cell death. We therefore investigated the ability of the H1 helix mutants to induce cell-cycle arrest and apoptosis in p53 null cell lines using adenoviruses expressing the p53 mutants together with GFP as a marker. All p53 proteins were expressed at equal levels and localized predominantly to the nucleus (data not shown). Compared to the GFP-only control, wild-type p53 expression induced both cell-cycle arrest and cell death, as seen by the reduced number of GFP-positive cells and the increased number of condensed apoptotic cells (Figure 2A). Interestingly, the interaction-impaired mutants EE, RR, EL, and LR also showed reduced numbers of GFP-positive cells, indicative of cell-cycle arrest, but failed to show apoptotic cells. This is consistent with a previous study in which the EL mutation was identified as a partial loss-of-function mutation with a selective apoptosis defect (Ludwig et al., 1996). In contrast, the cell cultures infected with the hyperactive mutant RE or the combination EE+RR displayed strongly elevated numbers of apoptotic cells, suggesting that the core domain interaction strength influences the outcome of p53 activation: weak interactions result in selective cell-cycle arrest and strong interactions in preferential induction of apoptosis.

Detailed cell-cycle profiling by flow cytometry confirmed that the interaction-impaired mutants EE, RR, EL, and LR induced cell-cycle arrest in the absence of apoptosis (Figure 2B; Figure S1E). Whereas RR, EL, and LR evoked an increase in both the G1 and G2/M populations, the EE mutant caused a selective increase in G1 that was sufficient to prevent accumulation in G2/M following nocodazole treatment (Figure 2C). In

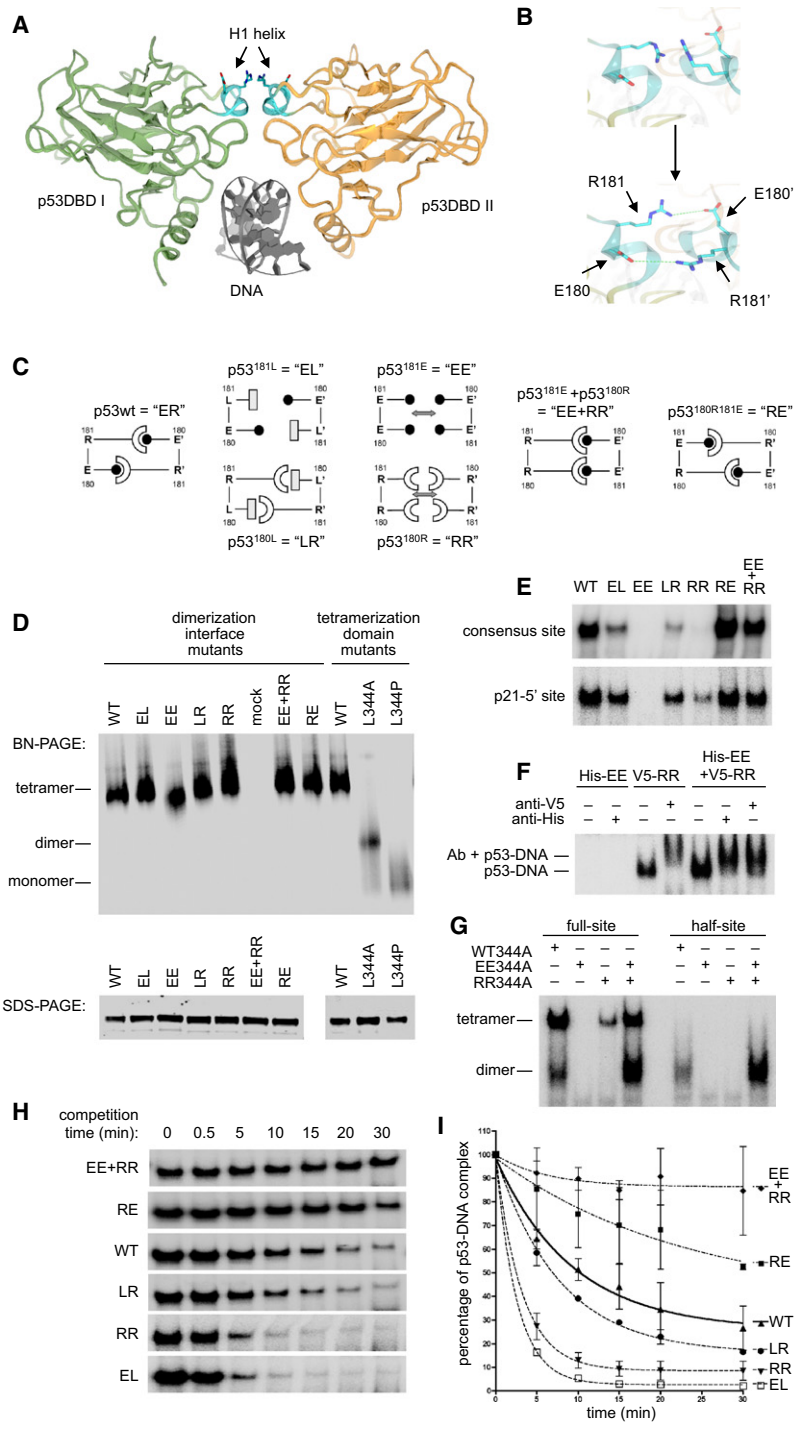

Figure 1. p53 H1 Helix Interactions Influence DNA Binding of Full-Length p53 In Vitro

(A) Structure of two p53 DNA-binding "core" domains (p53DBD I and II) in contact with a consensus binding sequence (Protein Data Bank ID code 2ADY) (Kitayner et al., 2006). The intradimer protein-protein interface involves the short H1 helix (cyan).

(B) View of the dimerization interface. Depicted is the conformation in the crystal (top) and a different Arg rotamer highlighting the stabilization of the dimerization interface by a double intermolecular salt bridge between residues E180 and R181 of each monomer (bottom).

(C) Schematic representation of the dimerization patterns of wild-type p53 "ER" and the H1 helix mutants in this study.

(D) Tetramerization of H1 helix mutants. In vitro translated ^{35}S-labeled p53 full-length proteins containing the indicated H1 helix mutations (EE, EL, RR, LR, RE, and EE+RR) or tetramerization domain mutations (L344A and L344P) were separated by blue native polyacrylamide gel electrophoresis (top panel) or SDS-PAGE (immunoblot, bottom panel).

(E) EMSA of in vitro translated p53 full-length proteins and ^{32}P-labeled dsDNA containing the p53 consensus response element or the 5′ binding site in the p21 promoter.

(F) EMSA of His-tagged EE and V5-tagged RR proteins with the ^{32}P-labeled consensus dsDNA. Anti-His and anti-V5 antibodies were added to the reaction mixture for supershift analysis.

(G) The dimeric L344A tetramerization domain mutant p53 protein was generated without (WT344A) and with H1 helix mutations (EE344A and RR344A) by in vitro translation. EMSA with ^{32}P-labeled dsDNA containing a full consensus response element (20-mer, "full-site") or a decameric "half-site."

(H and I) EMSA showing dissociation of the indicated p53 proteins from ^{32}P-labeled consensus dsDNA upon addition of a 100-fold excess of the same oligonucleotide lacking ^{32}P. Shown is the mean ± SD of two independent experiments.

stark contrast, the hyperactive RE mutant and the combination of the two apoptosis-deficient mutants EE and RR induced earlier caspase activation and higher levels of cell death than wild-type p53 (Figures 2A, 2B, 2D, and 2E). The functional apoptosis rescue was not restricted to the combination EE+RR, but was always observed when an E180 mutant (LR, RR) was combined with an R181 mutant (EL, EE), indicating that H1 helix interactions determine the apoptotic potential (Figure 2F). Furthermore, all H1 helix mutants function in a dominant-negative manner to inhibit apoptosis when coexpressed with wild-type p53 (Figure 2F). Acquisition of an H1 helix mutation in one p53 allele during tumor development could therefore compromise the activity of the remaining wild-type allele in a similar way as it has been reported for other classes of p53 mutations. Combined, these experiments demonstrate that strong H1 helix interactions are essential for apoptosis induction and that changes in interaction strength can alter the decision between cell-cycle arrest and apoptosis.

H1 Helix Interactions Are Essential for Conformational Activation of Bax and Bak

Apoptotic functions of p53 include a nuclear role as a transcription factor that activates expression of target genes and

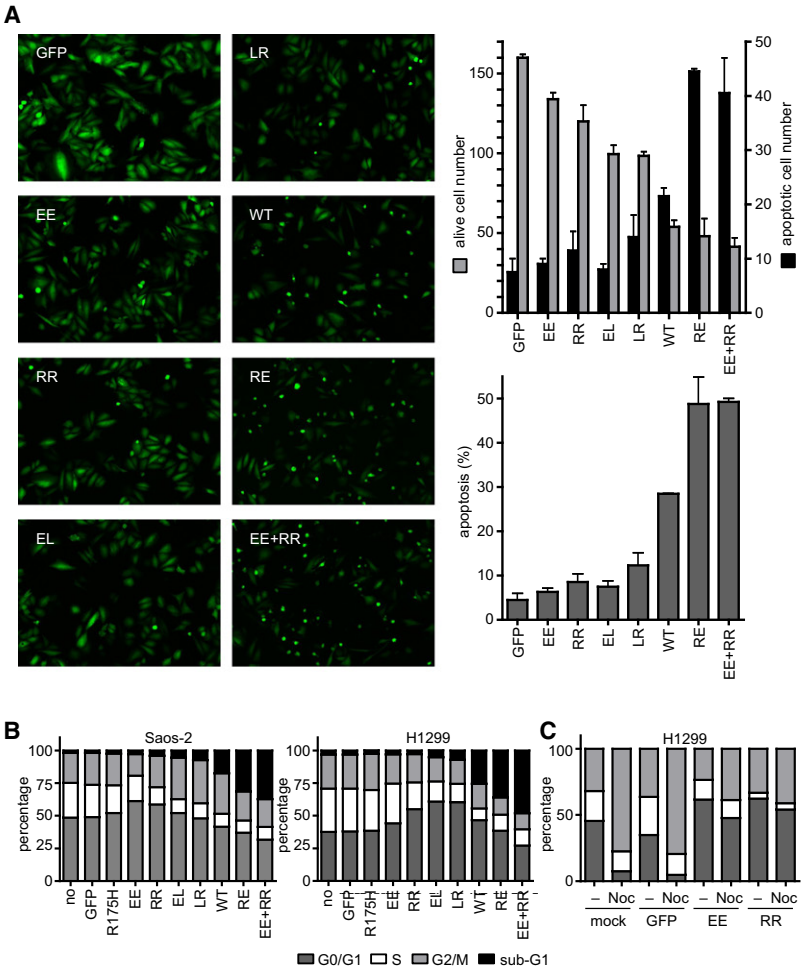

Figure 2. p53 DNA Binding Cooperativity Correlates with Apoptosis Induction

(A) Morphology of Saos-2 cells 30 hr following infection with adenoviruses coexpressing GFP and the indicated p53 proteins. Top right: number alive and apoptotic cells per field of view; lower right: percentage of apoptotic cells (mean ± SD).

(B and C) Cell-cycle profiles of Saos-2 cells 24 hr or H1299 cells 38 hr following infection with adenoviruses expressing the indicated p53 proteins.

(C) The cells were treated as indicated with nocodazole (40 ng/ml) for the last 12 hr to stimulate accumulation of proliferating cells in G2/M.

(D) Caspase-Glo 3/7 activity assay 24 hr following expression of p53 in Saos-2 cells. RLU, relative light units. Results are presented as mean ± SD.

(E) Immunodetection of the caspase-3 cleavage product in Saos-2 cells.

(F) Functional rescue by complementation of apoptosis-defective H1 helix mutants. Saos-2 cells were coinfected with equal amounts of two adenoviruses and apoptosis was quantified by caspase-3/7 activity measurement after 24 hr. The color intensity linearly correlates with caspase-3/7 activity.

(G) Saos-2 cells were infected for 9 hr with adenoviruses expressing the indicated p53 proteins. Mitochondria were purified by subcellular fractionation. Fifteen micrograms of mitochondrial (M), cytosolic (C), and total cellular (L) protein was separated by SDS-PAGE and subjected to immunoblotting.

(H) Total cellular lysates prepared 24 hr after infection as in (G) were immunoprecipitated with antibodies specific for Bak and Bax in their activated conformation. Precipitated proteins and total cellular lysates were separated by SDS-PAGE and subjected to immunoblotting. See also Figure S1.

a nonnuclear role in the cytoplasm and mitochondria involving p53 translocation to the outer mitochondrial membrane (Chipuk and Green, 2006). Despite their apoptosis defect, EE and EL were detected in purified mitochondrial fractions at similar levels as the wild-type protein and the strongly apoptotic RE mutant (Figure 2G). The absence of proliferating cell nuclear antigen (PCNA) in the mitochondrial extracts excluded nuclear contamination as a source of p53 in these fractions.

The endpoint of p53's mitochondrial action is the activation of the BH123 proteins Bax and Bak to allow mitochondrial outer-membrane permeabilization and release of apoptogenic factors triggering the activation of caspases and the apoptotic demise of the cell. The activation of Bax and Bak requires a conformational change that results in the exposure of the hidden BH3 domain as a prerequisite for self-oligomerization. To detect conformational activation, Bax and Bak proteins were immunoprecipitated from mutant p53-transfected Saos-2 cells with conformation-specific antibodies (Figure 2H). Substantial Bax and Bak activation was only induced by wild-type p53 and RE. We concluded that H1 helix mutations do not affect mitochondrial localization but rather the subsequent steps involved in Bax and Bak activation which were recently linked to p53's nuclear function (Chipuk and Green, 2006). In the following, we therefore focused our

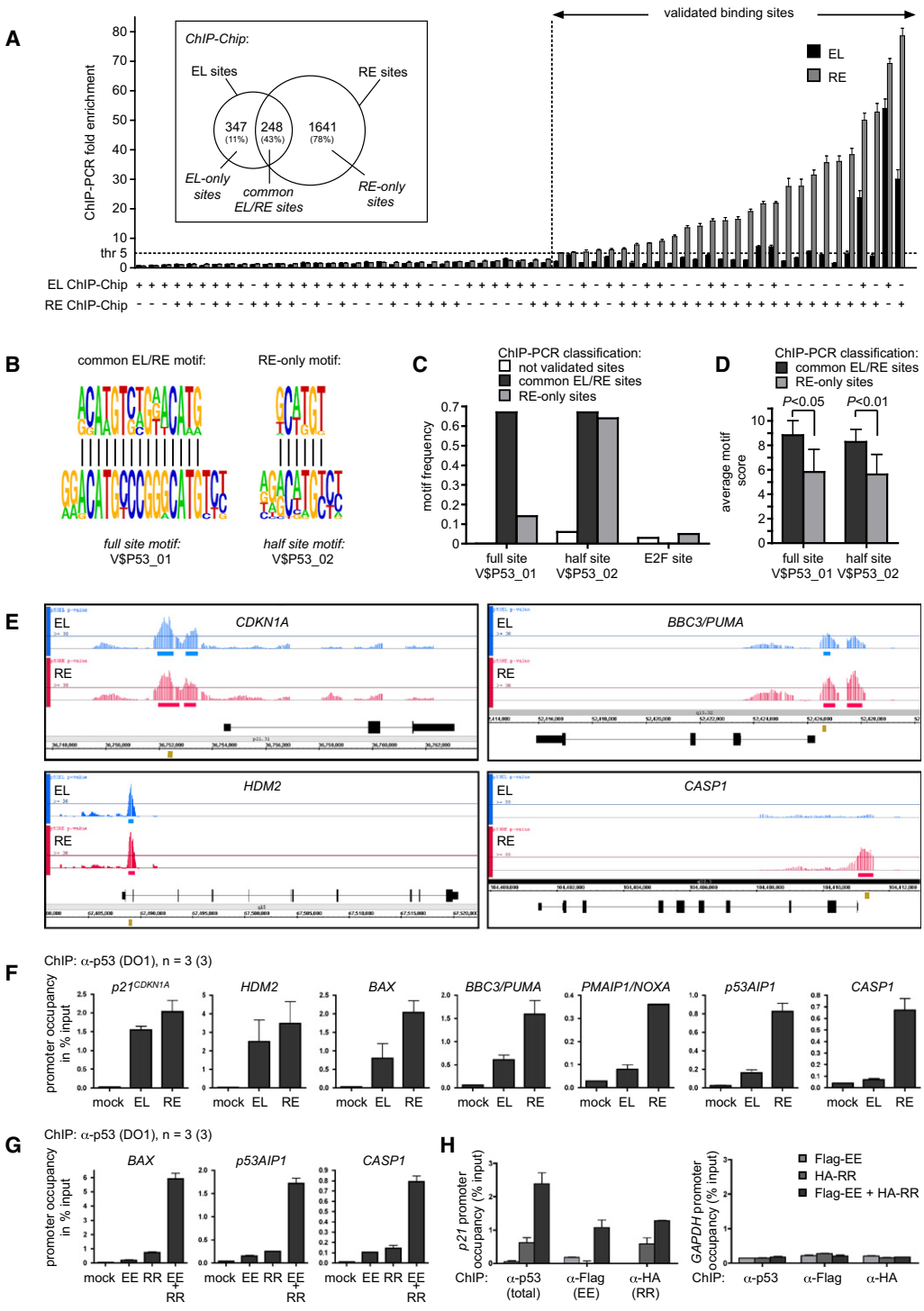

Figure 3. Role of p53 DNA Binding Cooperativity for In Vivo DNA Binding

(A) ChIP-Chip analysis was used to identify p53-binding sites in Saos-2 cells expressing the H1 helix mutant EL or RE compared to mock cells (Table S2). Sixty-one of these BS were randomly chosen for validation by ChIP-PCR. The identification of each site on EL and/or RE arrays is shown on the x axis. Reported is the fold enrichment of p53 (EL or RE) at this genomic position compared to mock as determined by ChIP-PCR. Inset: number and validation rate (in %) of EL and RE sites identified by ChIP-Chip. Results are presented as the mean ± SD.

(B) De novo motif discovery in validated common EL/RE and RE-only binding sequences. Twenty-meric and decameric consensus motifs are shown for comparison.

further analysis on the transcriptional activity of the H1 helix mutants.

In Vivo DNA Binding of H1 Helix Mutants

To measure the in vivo DNA-binding activity of H1 helix mutants in an unbiased manner, we used promoter arrays containing over 4.6 million probes tiled through over 25,500 human promoter regions (Affymetrix GeneChip Human Promoter 1.0R Array; minimum promoter coverage: 7.5 kb upstream through 2.45 kb downstream of the transcriptional start site; TSS). For this purpose, Saos-2 cells were infected with adenoviruses expressing either the H1 helix mutant EL or RE while mock-transfected cells served as internal controls. Cells were harvested 18 hr after infection when apoptosis had not yet occurred (Figure S1E). All ChIP-Chip experiments were done in triplicate, and binding sites (BS) were identified applying a statistical threshold of $p < 0.001$. A total of 595 BS were identified for EL and 1889 for RE (Table S2). A comparable analysis with wild-type p53 yielded 812 BS (data not shown). Twenty-eight of 61 (46%) randomly chosen BS showed a more than 5-fold enrichment for RE in ChIP-PCR validation experiments (Figure 3A; Table S3). The validation rate for EL sites was substantially lower (28%) than for the RE sites (60%) comprising mainly those BS which were also identified on the RE arrays (Table S3). Furthermore, all validated BS were bound stronger by RE than by EL, and not a single BS was identified that recruited EL but not RE. p53 BS can therefore be divided into ''common EL/RE'' sites and ''RE-only'' sites. Based on our experimental validation rate, we predict approximately 100 common and 1250 RE-only BS in the promoter regions of the human genome and concluded that DNA binding cooperativity strongly increases the number of p53 BS.

Functional annotation of common EL/RE sites with GATHER (http://gather.genome.duke.edu) revealed a significant enrichment (p value < 0.01, Bayes factor > 20) for the Gene Ontology (GO) terms ''response to stress'' and ''regulation of cell cycle'' (Table S4). The GO terms ''programmed cell death/apoptosis'' and ''regulation of programmed cell death/apoptosis'' were only significantly enriched among the RE-only sites. In both common and RE-only sites, the p53 consensus sequence (TRANSFAC M00272.p53) was found to be the most significantly enriched transcription factor binding motif. However, whereas 111 hits were found in the list of common sites, 543 hits were found in the list of RE-only sites. Together with the predicted number of true binding sites (~100 common and ~1250 RE-only sites), this implies that most common sites contain a consensus-like p53 binding motif, whereas more than 50% of RE-only sites have a BS that deviates from the consensus.

When using the ChIP-PCR-validated BS (shown in Figure 3A) for de novo motif discovery, we identified a p53 consensus-like binding motif (ACATGTCTGAACATG; Figure 3B; Table S5) in all validated common EL/RE sites. In contrast, in the list of validated RE-only sites, we only discovered a short motif (GCWTGT; Figure 3B; Table S5) resembling the core of a p53 half-site. Similarly, the p53 full-site motif (V$P53_01) was strongly enriched in the set of validated common sites but not in the validated RE-only sites. In contrast, the p53 half-site motif (V$P53_02) was found with equal frequency in all validated binding sites (Figure 3C). In both cases, the average motif score as a measure of similarity to the consensus was significantly lower among the validated RE-only sites (Figure 3D), indicating that RE tolerates mismatches to the consensus binding site better than EL. Another explanation for the absence of 20-meric full sites in RE-only sequences despite the presence of decameric half-sites are spacer elements that separate two half-sites. Applying a spacer-tolerant algorithm, we indeed identified spacer-containing full sites more frequently in RE-only than in common EL/RE sequences (Figures S2B and S2C). Together, these results suggest that the sequence requirements for recruitment of RE are less stringent than for EL. Consistently, in vitro DNA binding data demonstrated specific enhancement of p53 binding to lower-affinity and spacer-containing BS by increased DNA binding cooperativity (Figures S2A and S2D). Interestingly, the response elements in target genes of the apoptotic program are often lower-affinity BS frequently containing mismatches to the consensus (Riley et al., 2008).

When analyzing the binding profiles of H1 helix mutants on individual p53 target genes, it can be clearly seen that both mutants bind similarly to the $p21^{CDKN1A}$ and *HDM2* promoter but that recruitment to the promoters of the proapoptotic genes *BBC3*/*PUMA*, *CASP1*, *PMAIP1*/*NOXA*, and *BAX* exceeds the stringent threshold only in the case of RE (Figure 3E; Figures S2E and S2F). ChIP-PCR analysis of individual p53 target genes confirmed that the promoter occupancy was particularly different on proapoptotic gene promoters (*BAX*, *BBC3*/*PUMA*, *PMAIP1*/*NOXA*, *p53AIP1*, *CASP1*; Figure 3F). To confirm that the differential DNA binding characteristics of H1 helix mutants are truly due to interaction defects, we also analyzed functional complementation of the two most severely affected p53 mutants EE and RR. Both mutants on their own were strongly impaired in binding to p53 target genes, as expected from the overall negative (EE) or positive (RR) charge of the H1 helix and the in vitro DNA binding data. However, EE and RR mutually enhanced their promoter binding activity, strongly suggesting that in vivo DNA binding is determined by the interaction of the H1 helices (Figures 3G and 3H). Increased DNA binding cooperativity due to strong H1 helix interactions therefore enables p53 recruitment to promoters of proapoptotic genes, which are not efficiently bound in the absence of cooperative DNA binding.

(C and D) Frequency and average motif scores of the TRANSFAC motifs V$P53_01 (full site), V$P53_02 (half-site), and V$E2F_01 (E2F site as a control) in the binding sequences of (A). Results are presented as the mean ± SD.

(E) Genome browser view of EL and RE binding to individual p53 target genes as determined by ChIP-Chip analysis. Shown are the transformed p value averages of three array hybridizations. Genomic regions exceeding the statistical threshold p value of 0.001 are shown as horizontal bars. Yellow bars show the regions used for validation by ChIP-PCR.

(F) ChIP-PCR analysis of H1 helix mutant binding to selected p53 target genes. Results are presented as the mean ± SD.

(G and H) ChIP-PCR analysis of Flag-tagged EE and HA-tagged RR binding to the $p21^{CDKN1A}$ and *GAPDH* promoters using α-p53, α-Flag, or α-HA antibody. Shown is the mean ± SD for three independent experiments with three PCR replicates each, n = 3(3). See also Figure S2.

Gene Expression Profiling of H1 Helix Mutants

To characterize the transactivation function of H1 helix mutants in an unbiased manner, we performed gene expression profiling with cDNA microarrays. Saos-2 cells were infected with adenoviruses expressing the p53 proteins EE, EL, WT, and RE, which span the entire spectrum of apoptotic activity. A total of 186 genes were induced by wild-type p53 more than 3-fold 18 hr after infection (Figure 4A; Table S6). As expected from the weak DNA-binding activity of EE, the gene expression profile of EE-expressing cells was most similar to the GFP control sample. Based on our chromatin immunoprecipitation data, we expected RE to transactivate more genes than EL. However, the sets of activated genes appeared mutually exclusive, so two clusters of target genes could be distinguished: class I genes preferentially activated by the EL mutant with impaired DNA binding cooperativity, and class II genes selectively induced by the hyperactive mutant RE. Class I genes include $p21^{CDKN1A}$ and *HDM2* as key players of cell-cycle arrest and apoptosis inhibition, whereas class II genes include the proapoptotic genes *NOXA* (*PMAIP1*) and *CASP1* (validation qRT-PCR in Figure 4B).

Similarly, luciferase reporter assays demonstrated the $p21^{CDKN1A}$ promoter to be preferentially activated by H1 helix mutants with low interaction strength (RR, LR, EL), whereas the proapoptotic *BAX* and *p53AIP1* promoters were activated better by the p53 proteins WT, RE, and EE+RR (Figure 4C). Reduced transactivation of $p21^{CDNK1A}$ and *HDM2* by RE and EE+RR appeared paradoxical, considering efficient binding of these mutants to the promoters. A detailed analysis of the $p21^{CDNK1A}$ gene confirmed efficient binding of RE to the 5′ and 3′ p53 binding sites in the $p21^{CDNK1A}$ promoter, which even exceeded binding of EL (Figure S3A). Histone H3 and H4 panacetylation as well as H3K4 trimethylation were comparable for both p53 mutants. Recruitment of RNA polymerase II to the TSS and throughout the gene was lower in the case of RE. Lower RNA polymerase binding was similarly observed at the TSS of the *HDM2* promoter but not the *CASP1* promoter (Figure S3B). Higher levels of RE binding to the $p21^{CDNK1A}$ promoter but equal histone modification levels and reduced RNA pol II binding indicate an impaired coupling of RE to polymerase, possibly due to insufficient recruitment of coactivators. In addition, expression of transactivation-competent but not transactivation-deficient p53 inhibited the expression of a Gal4-dependent reporter driven by a fusion protein consisting of the Gal4-DNA-binding domain and the transactivation domain of p53 (Figure S3C). Because this effect was much stronger in the presence of RE than of EL, we concluded that RE, presumably because of its binding to many more sites in the genome than EL, causes a relative deficiency of coactivators, which results in a lower transactivation of $p21^{CDNK1A}$.

These data raised the question of whether RE is a stronger inducer of apoptosis than EL because of its ability to better activate proapoptotic genes or because it induces lower levels of antiapoptotic p21. Knockdown of p21 expression, however, did not result in apoptosis in EL-transfected cells, indicating that it is not the high-level induction of p21 but rather the defect in transactivating proapoptotic targets that limits apoptosis induction in the absence of DNA binding cooperativity (Figures S3D and S3E).

Furthermore, time course analysis of p53 target proteins following EL and RE expression indicated that EL primarily induced p21 and Hdm2 expression whereas RE induced strong expression of the proapoptotic Noxa, Bax, and Puma proteins, indicating intrinsically different target gene spectra of the two mutants (Figure 4E). Importantly, this difference was already observed at the earliest time points when p53 levels were lower than in p53 wild-type U2OS cells after DNA damage (Figures 4D and 4E). Similar to EL, the RR mutant also strongly activated p21 and Hdm2 (Figure 4F). However, coexpression of RR with the transcriptionally mostly inactive EE mutant shifted the target selectivity to Noxa and Bax, resulting in caspase-3 and PARP cleavage. Phosphorylation of key serine residues (S15, S20, S46, S392) was comparable for all mutants and could not account for the different apoptotic activities (data not shown). These findings were further confirmed in H1299 cells with inducible p53-ER^{TAM} constructs carrying the EL and RE mutations expressed at physiological levels (Figures S4A–S4H).

DNA Binding Cooperativity Enhances Apoptosis in Response to DNA Damage

Interestingly, in the H1299 p53-ER^{TAM} system, the difference between EL and RE became even more pronounced following additional treatment of these cells with the DNA-damaging agent doxorubicin, suggesting a role for DNA binding cooperativity in the DNA damage response (Figures S4E–S4H). Likewise, in Saos-2 cells transfected with the panel of H1 helix mutants, basal and DNA damage-induced levels of apoptosis directly correlated with cooperativity (Figures 5A–5C). To confirm these findings, we investigated p53 knockout HCT116 colon cancer cells that were reconstituted with our panel of H1 helix mutants. The p53 mutants were expressed at physiological levels and were similarly phosphorylated and stabilized in response to 5-fluorouracil (5-FU) (Figure 5D). Like typical loss-of-function p53 mutants (data not shown), the most inactive mutant EE was expressed at higher levels. Binding of p53 to the proapoptotic target genes *FAS* and *FDXR* was weak in unstressed cells and strongly induced 6 hr after 5-FU treatment in a cooperativity-dependent manner (Figure 5E). Transactivation of *FAS* and *FDXR* (Figure 5F) and apoptosis induction (Figures 5G and 5H) were similarly determined by DNA binding cooperativity. We therefore concluded that DNA binding cooperativity determines the extent of apoptosis in response to DNA damage.

The apoptotic function of p53 is stimulated in response to DNA damage by a number of posttranslational modifications and cofactors. For example, phosphorylation of serine 46 provides a docking site for the prolyl isomerase Pin1, which displaces the apoptosis inhibitor iASPP from p53 to promote cell death (Mantovani et al., 2007). This mechanism can be mimicked by the 46F mutation, which enhances p53's apoptotic function (Nakamura et al., 2006). Whereas the 46F mutation increased the apoptotic function of both p53 WT and EL, *NOXA* expression and basal as well as DNA damage-induced levels of apoptosis remained substantially lower for EL (Figures S4I–S4K). Furthermore, overexpression of ASPP2, which is known to stimulate p53 binding to proapoptotic target promoters (Samuels-Lev et al., 2001), increased the cytotoxicity of the H1 helix mutants, but the absolute amount of apoptosis

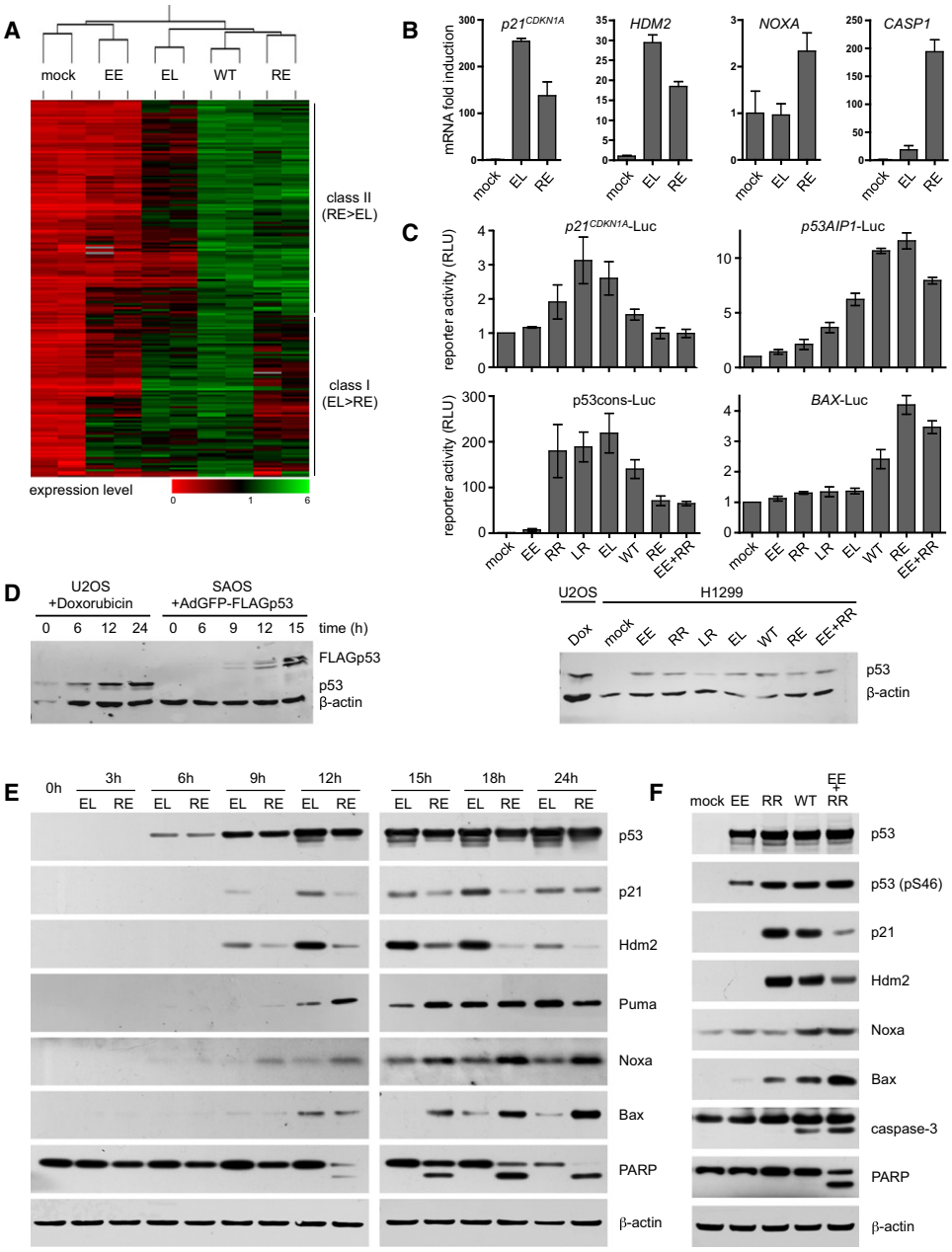

Figure 4. p53 DNA Binding Cooperativity Distinguishes Two Functionally Distinct Classes of p53 Target Genes

(A) Heat map depicting gene expression profiles of Saos-2 cells infected with adenoviruses expressing p53 wild-type and H1 helix mutants. Shown are the 186 genes that were induced by wild-type p53 more than 3-fold (Table S6). Two gene clusters are distinguished based on the relative induction by RE and EL.

(B) Validation by qRT-PCR. Samples as in (A) were analyzed for expression of target genes relative to the GFP-control sample (mock) and *GAPDH* as an internal standard. Shown is the mean ± SD (n = 3).

(C) Luciferase reporter assay of H1299 cells transfected with p53 expression and luciferase reporter plasmids. Luciferase activity was normalized to the mock control. Shown is the mean ± SD of two independent experiments with two replicates each. Immunoblot shows comparable expression of p53 in transfections and doxorubicin-treated U2OS cells.

(D–F) Immunoblots of doxorubicin-treated U2OS cells or Saos-2 cells infected with p53-expressing adenoviruses for the indicated time periods, 18 hr in (F). See also Figure S3.

was limited in the absence of DNA binding cooperativity (Figure S4L). Interestingly, ASPP2 could not further stimulate the apoptotic activity of the most highly cooperative mutant EE+RR, implying that ASPP2 functions by enhancing cooperativity. Together, these data suggest that DNA binding cooperativity is crucial for at least some posttranslational modifications and modulating cofactors to increase p53-mediated apoptosis in response to DNA damage.

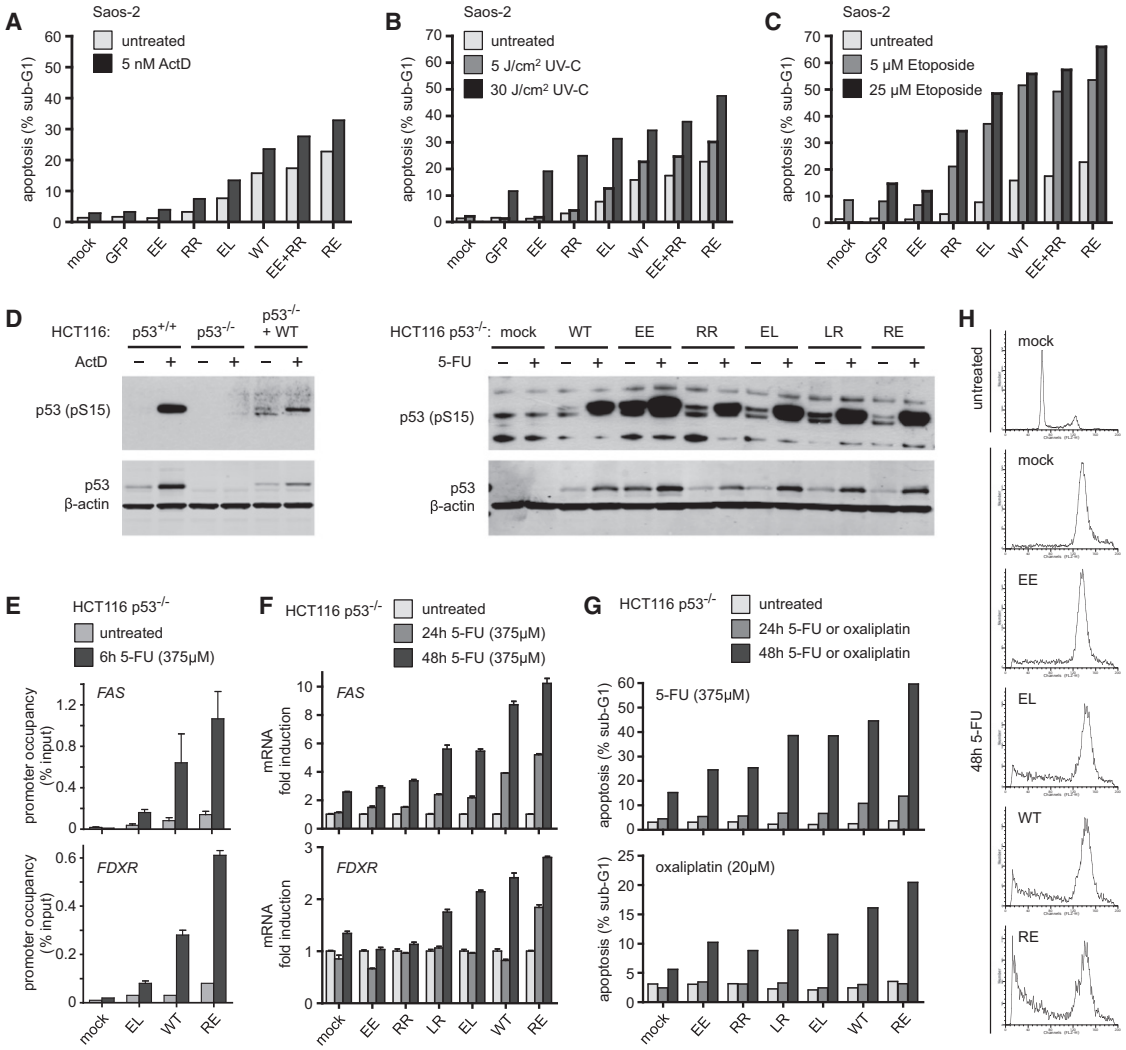

Figure 5. DNA Binding Cooperativity Is Crucial for Apoptosis in Response to DNA Damage

(A–C) Apoptosis of Saos-2 cells 24 hr following infection with indicated p53 adenoviruses in the absence or presence of DNA damage.

(D–H) p53 knockout ($p53^{-/-}$) HCT116 cells were reconstituted with wild-type or H1 helix mutant p53 by stable retroviral transduction.

(D) Immunoblots of parental ($p53^{+/+}$), $p53^{-/-}$, and p53-reconstituted HCT116 cells. For p53 activation, cells were treated for 24 hr with ActD (10 nM), 5-FU (375 μM), or oxaliplatin (20 μM).

(E) ChIP-PCR of p53 binding to *FAS* and *FDXR* promoters.

(F) qRT-PCR for *FAS* and *FDXR* mRNA.

(G and H) Apoptosis (sub-G1 population) (G) and cell-cycle profiles (H) of 5-FU-treated p53-reconstituted HCT116 cell lines. Results are presented as the mean ± SD. See also Figure S4.

DNA Binding Cooperativity Is Essential for p53's Tumor Suppressor Activity

The International Agency for Research on Cancer (IARC) TP53 Mutation Database, release R14, lists 146 tumor patients with somatic and 28 with germline mutations at positions E180 or R181. However, for rare somatic p53 mutations, the causal role for tumorigenesis is often unclear. We therefore focused our further studies on the mutations E180K (= KR), R181L (= EL), R181H (= EH), R181C (= EC), and R181P (= EP), which are genetically linked to tumor development in families with the hereditary Li-Fraumeni or Li-Fraumeni-like cancer susceptibility syndrome. DNA-protein complex stabilities in vitro were reduced for all five mutations in the order WT > EL > EH = EC > KR > EP (Figures 6A and 6B). The EP mutant showed no DNA binding and no significant activity in our further experiments. Considering that proline is known to kink or break helices, we assume that the EP mutation not only disrupts H1 helix interactions but has more profound effects on the folding of the DNA-binding domain. The remaining mutants displayed a defect in promoter binding and transactivation of apoptotic target genes (Figures 6C–6F), and this correlated with a loss of their apoptotic activity (Figures 6G and 6H). Similarly as seen for other low-cooperativity mutants (Figures 4B–4F), luciferase reporter constructs containing consensus-like p53 response elements were efficiently

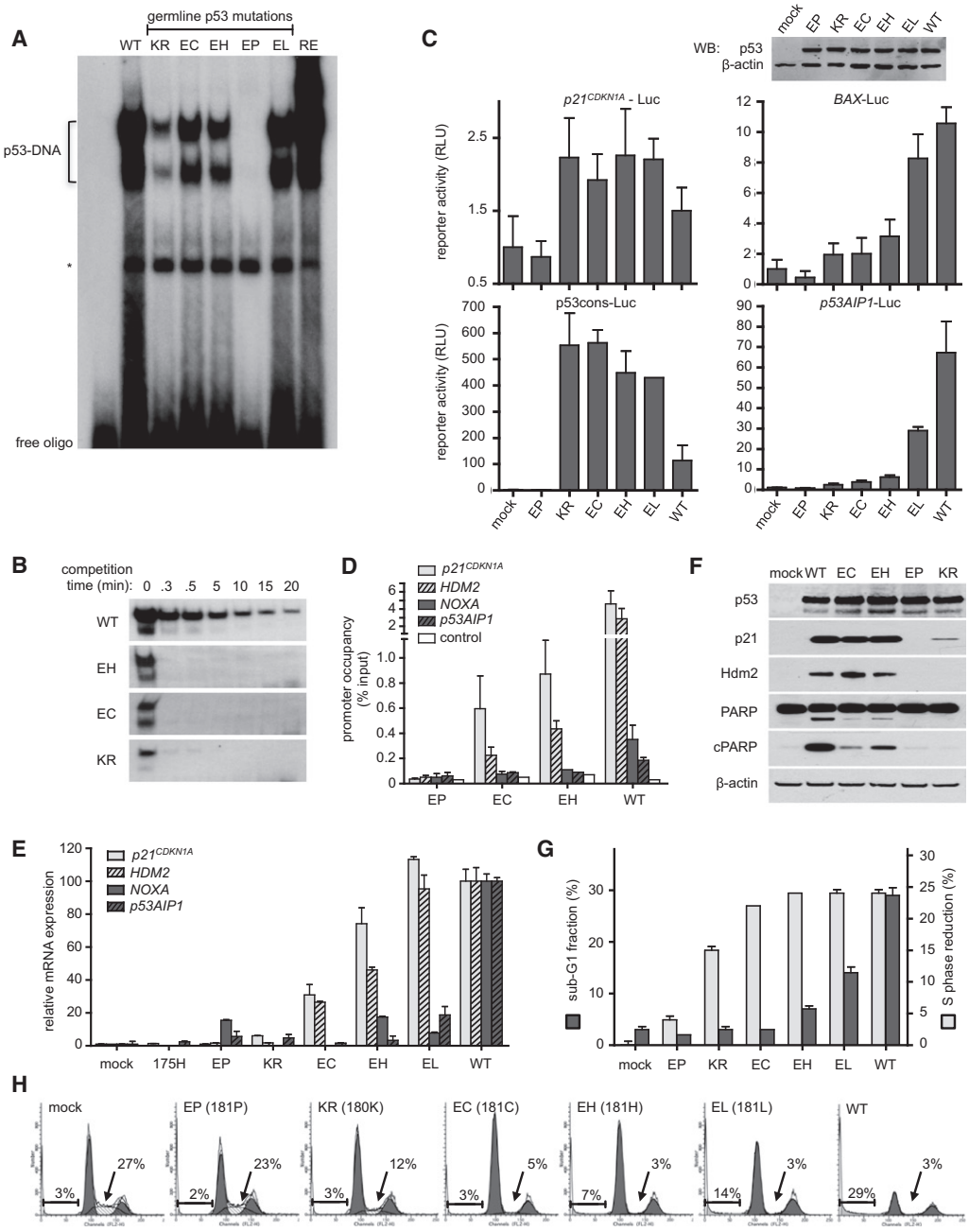

Figure 6. DNA Binding Cooperativity Is Essential for p53's Tumor Suppressor Activity

(A and B) EMSA of in vitro translated full-length p53 proteins and ^{32}P-labeled dsDNA containing the p53 consensus response element showing reduced DNA binding of p53 with germline H1 helix missense mutations.

(B) EMSA displaying dissociation of the indicated p53 proteins from ^{32}P-labeled consensus dsDNA upon addition of a 100-fold excess of the same oligonucleotide lacking ^{32}P.

(C) Luciferase reporter assay of H1299 cells transfected with p53 expression and luciferase reporter plasmids. Luciferase activity was normalized to the mock control. Shown is the mean ± SD of three transfections. Immunoblot shows comparable expression of all p53 constructs.

(D–H) Saos-2 cells were infected for 18 hr (D–F) or 34 hr (G and H) with adenoviruses expressing the indicated p53 proteins.

(D) ChIP-PCR.

(E) qRT-PCR.

(F) Immunoblot.

(G and H) Cell-cycle profiles determined by flow cytometry following propidium iodide staining. Results are presented as mean ± SD.

transactivated by these Li-Fraumeni mutants despite their lower than WT DNA binding affinity (Figures 6B and 6C). Consistently, the Li-Fraumeni mutants induced $p21^{CDKN1A}$ and caused a cell-cycle arrest. In the case of the KR mutant, p21 induction was lower than expected from the reporter activation study, which might reflect an unnatural activatability of the naked reporter plasmid compared to the endogenous gene in its chromatin context. In summary, four of the five Li-Fraumeni mutants showed the selective loss of apoptotic activity characteristic for reduced DNA binding cooperativity. As these mutations are genetically linked to cancer susceptibility in patients, we concluded that DNA binding cooperativity contributes to p53's tumor suppressor activity.

DISCUSSION

The structural basis for the DNA binding cooperativity of p53 is the interaction of H1 helices in the DNA-binding core domains. This interaction forms the symmetrical intradimer interface in the crystal structure of the DNA-bound core domain tetramer (Kitayner et al., 2006) and the solution dimerization interface as revealed by NMR spectroscopy (Klein et al., 2001). Mutational perturbation of this interface strongly impairs the cooperativity of in vitro DNA binding by isolated p53 core domains (Dehner et al., 2005). Considering that full-length p53 is assembled into a tetramer by strong interactions of the oligomerization domains, it remained unknown whether the H1 helix interaction interface plays a similar role in the context of the full-length p53 molecule. Our data demonstrate that the interaction of H1 helices is not required for the assembly of the tetramer. All H1 helix mutants formed tetrameric p53 molecules. Nevertheless, mutational perturbation of the interface strongly affected the DNA binding properties of p53 in vitro and in vivo, indicating that this interface determines DNA binding cooperativity also in the context of the tetrameric full-length p53 molecule.

As the H1 helix does not directly contribute to the DNA-binding surface of the core domain, indirect effects have to be considered to explain the influence of H1 helix mutations on DNA binding. Early attempts to model the tetrameric p53-DNA complex on the basis of the crystal structure by Cho et al. already indicated that the assembly of four core domains on a straight DNA strand with the experimentally predicted C2 symmetry would be accompanied by steric hindrance between the H1 helices (Cho et al., 1994). However, this steric clash is relieved and the H1 helices are optimally aligned for interaction when the DNA is bent toward the major groove away from the p53 core dimer, as has been observed in bending analyses (Balagurumoorthy et al., 1995), in the crystal structure of the DNA-bound tetramer (Kitayner et al., 2006), and by atomic force microscopy (Balagurumoorthy et al., 2002). DNA bending, however, is dependent on the nucleotide sequence. The CATG sequence within the p53 consensus response element is unusually flexible and exhibits extreme bending and kinking in many DNA-protein complexes (Balagurumoorthy et al., 2002; Olson et al., 1998). DNA binding affinity experiments have shown that p53 exhibits higher binding affinity for sites in cell-cycle control target genes than for sites in apoptosis target genes, and that these differences coincide with the prevalence of the highly flexible CATG in the cell-cycle control group (Weinberg et al., 2005). Efficient binding to non-CATG response elements (CAAG, CTTG, CTAG) may therefore require higher bending forces that depend on energetic stabilization provided by strong H1 helix interactions. Based on this model, interaction-impaired H1 helix mutants (EL, LR, RR) would be competent for forming a stable, optimally bent complex with a CATG response element but unable to bind the more rigid non-CATG sequences. In contrast, enhanced interactions (RE, EE+RR) would facilitate bending and binding to non-CATG sites. Indeed, electrophoretic mobility shift assays demonstrated efficient binding of EL, LR, and RR to the CATG sequences but only weak binding to non-CATG sites, in contrast to strong binding of RE and EE+RR to both CATG and non-CATG sites (Figure S2A). Thus, the H1 helix region would regulate DNA binding not by directly influencing the DNA contact surface but rather indirectly by providing additional energetic stabilization, which is required for p53 binding to sequences that are less easily bent, such as non-CATG response elements in many proapoptotic promoters.

In addition to the "dimer of dimers" structure of four DNA-bound core domains (Kitayner et al., 2006), recently an alternative "H14" binding mode of p53 was postulated on the basis of molecular dynamics simulations and the interaction interface in the asymmetric AB dimer of the p53-trimer DNA complex determined by X-ray crystallography (Ma and Levine, 2007). In contrast to the dimer of dimers structure, the H14 binding model nicely fits the recently described cryo-EM image of p53 (Okorokov et al., 2006). Whereas the H1 helices solely determine the intradimer interactions in the dimer of dimers structure, in the H14 binding mode they form a circular salt bridge which holds together all four core domains in the DNA-bound tetramer. Although our data reveal that H1 helix interactions play a role for intradimer interactions when tested in the context of the dimeric L344A mutant p53 molecule, they are also consistent with the proposed H14 structure, which is expected to be significantly stabilized by H1 helix interactions.

Interestingly, our study also indicates that cooperativity not only increases p53's apoptotic functions but also reduces its ability to activate cell-cycle arrest genes. This appears to be an indirect effect, as highly cooperative p53 molecules (RE and EE+RR) are efficiently recruited to the p53 response elements in the $p21^{CDKN1A}$ gene. According to our data, reduced transactivation results from an impaired coupling of promoter-bound p53 to the transcription machinery. One explanation is that highly cooperative p53 binds to so many sites in the genome that one or more, yet to be identified, coactivators become limiting, so that transactivation of genes such as $p21^{CDKN1A}$ is reduced. Hence, an increase in cooperativity shifts the cellular response away from cell-cycle arrest toward apoptosis (Figure 7).

Considering that the apoptotic function of p53 in response to DNA damage is regulated by posttranslational modifications or cofactor binding (Das et al., 2007; D'Orazi et al., 2002; Sykes et al., 2006; Taira et al., 2007; Tang et al., 2006), one question was whether cooperativity is upstream or downstream. First, we did not observe any differences in the basal and DNA damage-induced phosphorylation status of the p53 H1 helix mutants. However, given the multitude of posttranslational modifications that have been described for p53, we cannot

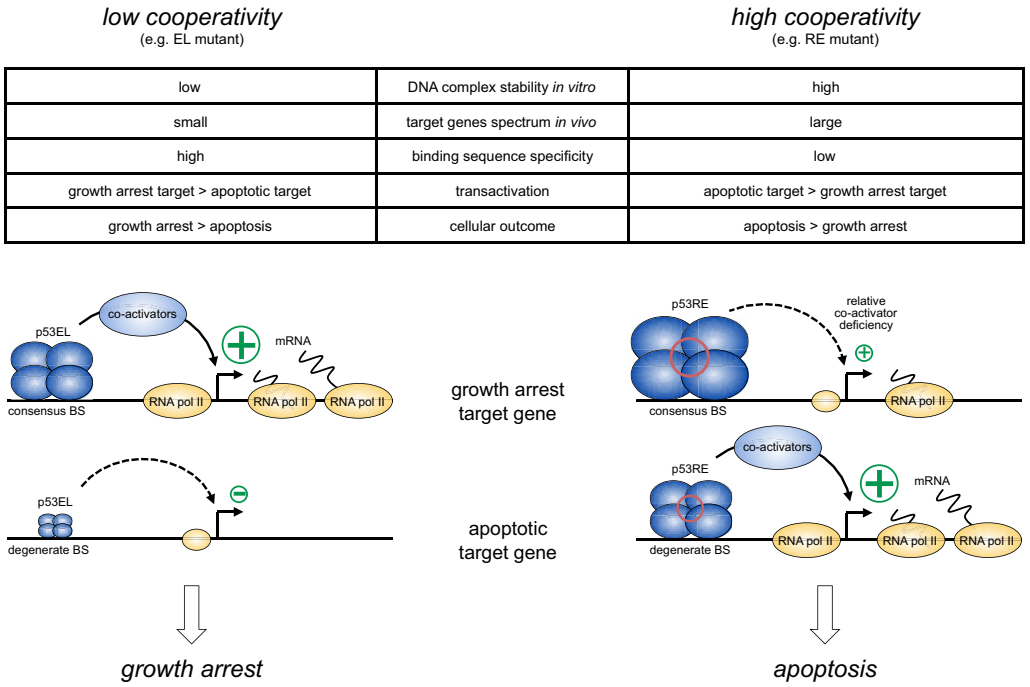

Figure 7. Role of DNA Binding Cooperativity for p53 Function

Model of the role of DNA binding cooperativity for target gene selection. The symbol size represents the amount of p53 and RNA pol II on the promoters as detected by ChIP. A red circle in the p53 tetramer symbolizes strong H1 helix interactions as the structural basis for DNA binding cooperativity.

exclude that other modifications might be affected in the set of mutants. In addition, various DNA-damaging agents, the activating 46F mutation, and expression of ASPP2 stimulated the apoptotic activity of the H1 helix mutants, but the resulting apoptosis level was in all cases determined by the extent of cooperativity. Together, these findings suggest that cooperativity is downstream in the p53 activating pathway. We therefore hypothesize that activating signals such as posttranslational modifications are upstream and translated into changes in DNA binding cooperativity causing p53 to switch from a weakly to a highly cooperative DNA binding factor. However, because DNA binding cooperativity cannot be directly measured in living cells at present, this hypothesis remains to be proven.

In general, tumor-derived point mutations in p53 fall into two classes: contact mutations affect p53 residues that directly interact with the DNA, whereas structural mutations cause local unfolding or global denaturation of the core domain. The H1 helix mutations described here represent a mechanistically distinct class of p53 mutations that affect a protein-protein interface in the quaternary structure of the p53-DNA complex. Mutations in this region have been identified as sporadic mutations in cancer patients (e.g., R181 to His; Leu, Pro, Cys, or E180 to Lys) as well as germline mutations in families with the Li-Fraumeni or Li-Fraumeni-like cancer susceptibility syndrome (IARC TP53 Mutation Database). Segregation of the cancer phenotype with the R181L (EL), R181C (EC), R181H (EH), and E180K (KR) mutations in Li-Fraumeni-like families, which all show a selective apoptotic defect (Figure 6), clearly indicates that impaired DNA binding cooperativity reduces p53's tumor suppressor activity. H1 helix interactions therefore contribute to the tumor suppressor function of p53 and could provide a therapeutic target to direct the outcome of p53 activation to either cell-cycle arrest or apoptosis.

EXPERIMENTAL PROCEDURES

Cell Culture and Viral Transduction

Cell lines were cultured in Dulbecco's modified Eagle's medium (Sigma) supplemented with 10% fetal bovine serum (Sigma) using standard conditions and procedures. Recombinant adenoviruses for p53 H1 helix mutants were generated with the AdEasy System (Stratagene). Cells were transduced with recombinant retro- and adenovirus as previously described (Cam et al., 2006).

Chromatin Immunoprecipitation and Genome-wide Promoter Analysis

Chromatin immunoprecipitations were performed as described (Cam et al., 2006). ChIP-Chip assays were performed with the p53 DO-1 antibody (Santa Cruz Biotechnology) on GeneChip Human Promoter 1.0R Arrays (Affymetrix) according to manufacturer recommendations. Detailed procedures for ChIP-PCR and ChIP-Chip can be found in Supplemental Experimental Procedures. The complete set of ChIP-Chip data has been deposited in EBI ArrayExpress (http://www.ebi.ac.uk/arrayexpress) under accession number E-MEXP-1748.

RT-PCR and Expression Profiling

Quantitative RT-PCR was performed as described (Cam et al., 2006). Primers and expression profiling procedures can be found in Supplemental Experimental Procedures. The complete set of microarray data has been deposited in EBI ArrayExpress (http://www.ebi.ac.uk/arrayexpress) under accession number E-MEXP-1209.

Additional experimental procedures are provided in Supplemental Information.

SUPPLEMENTAL INFORMATION

Supplemental Information includes Supplemental Experimental Procedures, four figures, and six tables and can be found with this article online at doi:10.1016/j.molcel.2010.02.037.

ACKNOWLEDGMENTS

We thank Moshe Oren, Bert Vogelstein, Trevor Littlewood, Yoichi Taya, Michael Schön, and Xin Lu for providing reagents, Michael Krause for assistance with microarrays, Justus Beck for mitochondrial localization experiments, Anna-Maria Maas for luciferase assays, Jochen Kuper for viewing and discussing p53 crystal structures, and Helmut Hänsel for help with bioinformatic data analysis. A.R. is supported by the Interdisciplinary Center for Clinical Research (IZKF), Würzburg, Germany. This work was funded by grants to T.S. of the Deutsche Forschungsgemeinschaft (Transregio TR17 Teilprojekt B2, Klinische Forschergruppe KFO210 STI 182/3-1, Forschungszentrum FZ82), Deutsche Krebshilfe (107904), and von Behring-Röntgen-Stiftung (57-0012).

Received: August 11, 2009
Revised: August 17, 2009
Accepted: February 16, 2010
Published: May 13, 2010

REFERENCES

Balagurumoorthy, P., Sakamoto, H., Lewis, M.S., Zambrano, N., Clore, G.M., Gronenborn, A.M., Appella, E., and Harrington, R.E. (1995). Four p53 DNA-binding domain peptides bind natural p53-response elements and bend the DNA. Proc. Natl. Acad. Sci. USA *92*, 8591–8595.

Balagurumoorthy, P., Lindsay, S.M., and Harrington, R.E. (2002). Atomic force microscopy reveals kinks in the p53 response element DNA. Biophys. Chem. *101-102*, 611–623.

Cam, H., Griesmann, H., Beitzinger, M., Hofmann, L., Beinoraviciute-Kellner, R., Sauer, M., Huttinger-Kirchhof, N., Oswald, C., Friedl, P., Gattenlohner, S., et al. (2006). p53 family members in myogenic differentiation and rhabdomyosarcoma development. Cancer Cell *10*, 281–293.

Chipuk, J.E., and Green, D.R. (2006). Dissecting p53-dependent apoptosis. Cell Death Differ. *13*, 994–1002.

Cho, Y., Gorina, S., Jeffrey, P.D., and Pavletich, N.P. (1994). Crystal structure of a p53 tumor suppressor-DNA complex: understanding tumorigenic mutations. Science *265*, 346–355.

Das, S., Raj, L., Zhao, B., Kimura, Y., Bernstein, A., Aaronson, S.A., and Lee, S.W. (2007). Hzf determines cell survival upon genotoxic stress by modulating p53 transactivation. Cell *130*, 624–637.

Dehner, A., Klein, C., Hansen, S., Muller, L., Buchner, J., Schwaiger, M., and Kessler, H. (2005). Cooperative binding of p53 to DNA: regulation by protein-protein interactions through a double salt bridge. Angew. Chem. Int. Ed. Engl. *44*, 5247–5251.

D'Orazi, G., Cecchinelli, B., Bruno, T., Manni, I., Higashimoto, Y., Saito, S., Gostissa, M., Coen, S., Marchetti, A., Del Sal, G., et al. (2002). Homeodomain-interacting protein kinase-2 phosphorylates p53 at Ser 46 and mediates apoptosis. Nat. Cell Biol. *4*, 11–19.

Kitayner, M., Rozenberg, H., Kessler, N., Rabinovich, D., Shaulov, L., Haran, T.E., and Shakked, Z. (2006). Structural basis of DNA recognition by p53 tetramers. Mol. Cell *22*, 741–753.

Klein, C., Planker, E., Diercks, T., Kessler, H., Kunkele, K.P., Lang, K., Hansen, S., and Schwaiger, M. (2001). NMR spectroscopy reveals the solution dimerization interface of p53 core domains bound to their consensus DNA. J. Biol. Chem. *276*, 49020–49027.

Ludwig, R.L., Bates, S., and Vousden, K.H. (1996). Differential activation of target cellular promoters by p53 mutants with impaired apoptotic function. Mol. Cell. Biol. *16*, 4952–4960.

Ma, B., and Levine, A.J. (2007). Probing potential binding modes of the p53 tetramer to DNA based on the symmetries encoded in p53 response elements. Nucleic Acids Res. *35*, 7733–7747.

Mantovani, F., Tocco, F., Girardini, J., Smith, P., Gasco, M., Lu, X., Crook, T., and Del Sal, G. (2007). The prolyl isomerase Pin1 orchestrates p53 acetylation and dissociation from the apoptosis inhibitor iASPP. Nat. Struct. Mol. Biol. *14*, 912–920.

Nakamura, Y., Futamura, M., Kamino, H., Yoshida, K., Nakamura, Y., and Arakawa, H. (2006). Identification of p53-46F as a super p53 with an enhanced ability to induce p53-dependent apoptosis. Cancer Sci. *97*, 633–641.

Okorokov, A.L., Sherman, M.B., Plisson, C., Grinkevich, V., Sigmundsson, K., Selivanova, G., Milner, J., and Orlova, E.V. (2006). The structure of p53 tumour suppressor protein reveals the basis for its functional plasticity. EMBO J. *25*, 5191–5200.

Olson, W.K., Gorin, A.A., Lu, X.J., Hock, L.M., and Zhurkin, V.B. (1998). DNA sequence-dependent deformability deduced from protein-DNA crystal complexes. Proc. Natl. Acad. Sci. USA *95*, 11163–11168.

Riley, T., Sontag, E., Chen, P., and Levine, A. (2008). Transcriptional control of human p53-regulated genes. Nat. Rev. Mol. Cell Biol. *9*, 402–412.

Samuels-Lev, Y., O'Connor, D.J., Bergamaschi, D., Trigiante, G., Hsieh, J.K., Zhong, S., Campargue, I., Naumovski, L., Crook, T., and Lu, X. (2001). ASPP proteins specifically stimulate the apoptotic function of p53. Mol. Cell *8*, 781–794.

Stiewe, T. (2007). The p53 family in differentiation and tumorigenesis. Nat. Rev. Cancer *7*, 165–168.

Sykes, S.M., Mellert, H.S., Holbert, M.A., Li, K., Marmorstein, R., Lane, W.S., and McMahon, S.B. (2006). Acetylation of the p53 DNA-binding domain regulates apoptosis induction. Mol. Cell *24*, 841–851.

Taira, N., Nihira, K., Yamaguchi, T., Miki, Y., and Yoshida, K. (2007). DYRK2 is targeted to the nucleus and controls p53 via Ser46 phosphorylation in the apoptotic response to DNA damage. Mol. Cell *25*, 725–738.

Tang, Y., Luo, J., Zhang, W., and Gu, W. (2006). Tip60-dependent acetylation of p53 modulates the decision between cell-cycle arrest and apoptosis. Mol. Cell *24*, 827–839.

Tidow, H., Melero, R., Mylonas, E., Freund, S.M., Grossmann, J.G., Carazo, J.M., Svergun, D.I., Valle, M., and Fersht, A.R. (2007). Quaternary structures of tumor suppressor p53 and a specific p53 DNA complex. Proc. Natl. Acad. Sci. USA *104*, 12324–12329.

Veprintsev, D.B., Freund, S.M., Andreeva, A., Rutledge, S.E., Tidow, H., Canadillas, J.M., Blair, C.M., and Fersht, A.R. (2006). Core domain interactions in full-length p53 in solution. Proc. Natl. Acad. Sci. USA *103*, 2115–2119.

Vousden, K.H., and Lane, D.P. (2007). p53 in health and disease. Nat. Rev. Mol. Cell Biol. *8*, 275–283.

Vousden, K.H., and Lu, X. (2002). Live or let die: the cell's response to p53. Nat. Rev. Cancer *2*, 594–604.

Weinberg, R.L., Veprintsev, D.B., and Fersht, A.R. (2004). Cooperative binding of tetrameric p53 to DNA. J. Mol. Biol. *341*, 1145–1159.

Weinberg, R.L., Veprintsev, D.B., Bycroft, M., and Fersht, A.R. (2005). Comparative binding of p53 to its promoter and DNA recognition elements. J. Mol. Biol. *348*, 589–596.